Atmos. Chem. Phys., 11, 7875–7891, 2011
www.atmos-chem-phys.net/11/7875/2011/
doi:10.5194/acp-11-7875-2011

Atmospheric Chemistry and Physics

Forest-atmosphere exchange of ozone: sensitivity to very reactive biogenic VOC emissions and implications for in-canopy photochemistry

G. M. Wolfe[1,*], J. A. Thornton[1], M. McKay[2,], and A. H. Goldstein[2]**

[1]Department of Atmospheric Sciences, University of Washington, Seattle, WA, USA
[2]Department of Environmental Science, Policy, and Management, University of California, Berkeley, CA, USA
[*]now at: Department of Chemistry, University of Wisconsin, Madison, WI, USA
[**]now at: California Air Resources Board, Sacramento, CA, USA

Received: 20 March 2011 – Published in Atmos. Chem. Phys. Discuss.: 3 May 2011
Revised: 15 July 2011 – Accepted: 23 July 2011 – Published: 4 August 2011

Abstract. Understanding the fate of ozone within and above forested environments is vital to assessing the anthropogenic impact on ecosystems and air quality at the urban-rural interface. Observed forest-atmosphere exchange of ozone is often much faster than explicable by stomatal uptake alone, suggesting the presence of additional ozone sinks within the canopy. Using the Chemistry of Atmosphere-Forest Exchange (CAFE) model in conjunction with summer noontime observations from the 2007 Biosphere Effects on Aerosols and Photochemistry Experiment (BEARPEX-2007), we explore the viability and implications of the hypothesis that ozonolysis of very reactive but yet unidentified biogenic volatile organic compounds (BVOC) can influence the forest-atmosphere exchange of ozone. Non-stomatal processes typically generate 67 % of the observed ozone flux, but reactions of ozone with measured BVOC, including monoterpenes and sesquiterpenes, can account for only 2 % of this flux during the selected timeframe. By incorporating additional emissions and chemistry of a proxy for very reactive VOC (VRVOC) that undergo rapid ozonolysis, we demonstrate that an in-canopy chemical ozone sink of $\sim 2 \times 10^8$ molec cm^{-3} s^{-1} can close the ozone flux budget. Even in such a case, the 65 min chemical lifetime of ozone is much longer than the canopy residence time of $\sim$2 min, highlighting that chemistry can influence reactive trace gas exchange even when it is "slow" relative to vertical mixing. This level of VRVOC ozonolysis could enhance OH and RO_2 production by as much as 1 pptv s^{-1} and substantially alter their respective vertical profiles depending on the actual product yields. Reaction products would also contribute significantly to the oxidized VOC budget and, by extension, secondary organic aerosol mass. Given the potentially significant ramifications of a chemical ozone flux for both in-canopy chemistry and estimates of ozone deposition, future efforts should focus on quantifying both ozone reactivity and non-stomatal (e.g. cuticular) deposition within the forest.

Correspondence to: J. A. Thornton
(thornton@atmos.washington.edu)

1 Introduction

Forest-atmosphere exchange of ozone (O_3) influences both atmospheric composition and biosphere productivity, with significant ramifications for air quality, ecosystem health and atmosphere-biosphere-climate feedbacks. Global chemical-transport models predict a global dry deposition flux of $\sim$1000 Tg(O_3) yr^{-1}, which is equal in magnitude to the sum of inputs from net chemistry (production – loss) and stratosphere-troposphere exchange (Stevenson et al., 2006). Deposition of ozone induces a range of biochemical and physiological changes in vegetation (Darrall, 1989; Zheng et al., 2002; Goumenaki et al., 2010), which can alter hydrocarbon emission profiles (Schade and Goldstein, 2002; Karl et al., 2005) and inhibit carbon sequestration (Ashmore, 2005; Matyssek et al., 2010; Zapletal et al., 2011; Bytnerowicz et al., 2008). A coupled chemistry-climate modeling study by Sitch et al. (2007) suggests that indirect radiative forcing associated with the limiting effect of ozone deposition on terrestrial net primary productivity is equal in magnitude to the direct forcing from tropospheric ozone. Stomatal uptake is thought to be the primary pathway for plant damage, leading to a suggested shift in risk assessment criteria

Published by Copernicus Publications on behalf of the European Geosciences Union.

from concentration-based metrics (e.g. accumulated total exposure) to a stomatal flux-based index (UNECE, 2004; Ashmore, 2005; Matyssek and Innes, 1999). Non-stomatal deposition can also be harmful; for example, reactive uptake to cuticular waxes may increase surface wetability and thus stomatal occlusion (Karnosky et al., 1999).

Typically, ozone deposition is quantified via above-canopy eddy covariance flux measurements (Fowler et al., 2009). While yielding a direct estimate of net forest-atmosphere exchange, such observations provide little conclusive information regarding the nature of underlying sources and sinks. Stomatal fluxes, usually calculated independently from observed water vapor fluxes (Monteith and Unsworth, 1990; Thom, 1975), generally account for only 30–70 % of the observed above-canopy ozone flux (Coe et al., 1995; Kurpius and Goldstein, 2003; Goldstein et al., 2004; Hogg et al., 2007; Fares et al., 2010a,b; Altimir et al., 2004, 2006; Rondon et al., 1993). The remaining "non-stomatal" portion of the ozone flux budget has been ascribed to a range of physical and chemical processes, including light-stimulated surface loss (Coe et al., 1995; Rondon et al., 1993), surface-mediated thermal decomposition (Cape et al., 2009), aqueous reactions in surface-accumulated liquid water (Altimir et al., 2006), and gas-phase reactions with biogenic volatile organic compounds (BVOC) (Fares et al., 2010a; Goldstein et al., 2004; Hogg et al., 2007; Kurpius and Goldstein, 2003) or nitric oxide (NO) (Dorsey et al., 2004; Duyzer et al., 2004) emitted from the ecosystem.

Current models of forest-atmosphere exchange generally assume that non-stomatal ozone flux is driven by surface losses and incorporate empirical parameterizations to correct for observed correlations with temperature, vapor pressure deficit, radiation and friction velocity (Wesely, 1989; Wesely and Hicks, 2000; Zhang et al., 2002, 2003; Bassin et al., 2004). This approach does not address the mechanisms underlying observed non-stomatal fluxes, which limits the predictive capability of models assessing differences across ecosystems and future changes within an ecosystem. Moreover, many of the hypothesized mechanisms exhibit similar meteorological signatures (e.g. BVOC emissions also vary with light and temperature), making it difficult to conclusively identify the nature of near-surface ozone sinks from the available data.

Homogeneous (gas-phase) chemistry within the canopy space has been proposed as another explanation for the "missing" ozone flux. This chemical ozone flux hypothesis is primarily based on a decade of observations at the University of California's Blodgett Forest Research Station (BFRS), a forest tower site situated in the western foothills of the Sierra Nevada. In an analysis of a single year of ozone flux observations (June 2000–May 2001), Kurpius and Goldstein (2003) demonstrated that stomatal uptake and non-stomatal deposition only account for ∼50 % of the summertime ozone flux observed above the BFRS canopy. The authors further showed that the remaining non-depositional flux exhibits strong temperature dependence similar to that of monoterpene emissions, leading to the conclusion that in-canopy reactions of ozone with unidentified BVOC drive this additional downward flux. Similar behavior has been observed in the longer-term dataset (2001–2006) as well (Fares et al., 2010a). Moreover, enhancements in O_3 fluxes coincided with observed increases in BVOC emissions during and after forest thinning in the summer of 2000, while stomatal deposition actually decreased (Goldstein et al., 2004). During summer 2003, Holzinger et al. (2005) observed substantial quantities of unidentified VOC oxidation products, some of which exhibited strong vertical gradients indicative of in-canopy production. The authors estimate a BVOC precursor emission rate of 13–66 $\mu mol\, m^{-2}\, h^{-1}$, which is 6–30 times the observed above-canopy monoterpene emission rate in that study. Such reactivity, if present, could enhance secondary organic aerosol formation (Hallquist et al., 2009) and, for alkene ozonolysis reactions, near-surface OH concentrations (Paulson et al., 1998, 1999). The existence of a chemical ozone flux would thus imply deficiencies in current BVOC emission inventories, as concentrations of currently measured reactive BVOC cannot fully account for the magnitude of the observed non-stomatal fluxes (Goldstein et al., 2004; Wolfe et al., 2011; Bouvier-Brown et al., 2009b).

To further explore the chemical ozone flux hypothesis, we have performed a series of sensitivity studies utilizing the **C**hemistry of **A**tmosphere-**F**orest **E**xchange (CAFE) model in conjunction with observations from the 2007 **B**iosphere **E**ffects on **Aer**osols and **P**hotochemistry **Ex**periment (BEARPEX). We choose to focus on this campaign because CAFE has been validated against this dataset, which represents the most comprehensive set of chemical observations available for BFRS. First, we provide a brief review of CAFE and detail the necessary modifications to the chemical mechanism. Central to this study is the incorporation of a chemical scheme for a generic very reactive BVOC. We then describe results from model runs where the emission rate and chemistry of this compound and its oxidation products are varied to probe the potential impacts on above-canopy ozone fluxes and in-canopy photochemistry. We focus in particular on radical cycling, secondary chemistry and the effects of canopy microclimate. By using a detailed model to more fully explore these implications, we therefore provide avenues for further observational tests of this hypothesis.

2 Methods

2.1 The CAFE model

CAFE is a 1-D steady-state chemical transport model described in detail elsewhere (Wolfe and Thornton, 2011; Wolfe et al., 2011). Briefly, the model domain consists of 86 vertical layers of varying thickness that extend from the

ground through a simulated forest canopy and up to the top of the atmospheric boundary layer (800 m). For the currently modeled canopy (Sect. 2.2), 36 of these layers are within the canopy. Within each layer, the 1-D time-dependent continuity equation is solved to determine the rate of change for all chemical species:

$$\frac{\partial C(z)}{\partial t} = P(z) + L(z) + E(z) + D(z) + A(z) - \frac{\partial F(z)}{\partial z} \quad (1)$$

Terms on the right respectively represent rates of chemical production (P), chemical loss (L), emission (E), deposition (D), horizontal advection (A), and vertical turbulent flux divergence ($\partial F/\partial z$), all of which are a function of altitude (z). The CAFE chemical mechanism is based on a subset of the Master Chemical mechanism (MCM) v3.1 (Jenkin et al., 1997; Saunders et al., 2003), with modifications as discussed elsewhere (Wolfe and Thornton, 2011; Wolfe et al., 2011). BVOC emissions, including isoprene, 2-methyl-3-buten-2-ol (MBO), methyl chavicol and a suite of monoterpenes and sesquiterpenes, are parameterized as a function of vegetation type, leaf area density, temperature and light following standard algorithms (Guenther et al., 1995) and observed leaf-level emissions for this site (Bouvier-Brown et al., 2009b). Soil NO emissions are assumed as $3\,\mathrm{ngN\,m^{-2}\,s^{-1}}$, which is consistent with previous NO flux measurements in this region (Bytnerowicz and Fenn, 1996) and with soil NO fluxes observed at this forest in 2009 (E. Browne, personal communication, 2010). Deposition follows the standard resistance parameterization (Wesely, 1989; Wesely and Hicks, 2000) and includes stomatal, non-stomatal and ground deposition for 35 species. Parameters for stomatal uptake have been adjusted to optimize agreement with observationally-derived stomatal conductances (Wolfe and Thornton, 2011). Advection is treated as a simple first-order process of mixing with "background air" (Dillon et al., 2002) and is used to help constrain chemical concentrations to observations. Meteorological profiles (i.e. temperature, friction velocity, radiation, etc.) are held constant throughout a model run according to measured and/or parameterized values; CAFE does not include an explicit online calculation of these variables. The model is initialized with chemical concentrations and run to steady state using operator splitting for the diffusive and chemical terms (emission, deposition and advection are also included in the chemical operator). Diffusion is solved with a Crank-Nicolson scheme and chemistry with a forward Euler scheme, both with a time step of 0.05 s. Fluxes (F) and exchange velocities (V_{ex}) are calculated from modeled concentration profiles ($C(z)$) via

$$F(z) = -K(z)\frac{\Delta C(z)}{\Delta z} \quad (2)$$

$$V_{ex}(z) = F(z)\big/C(z) \quad (3)$$

where $K(z)$ is the prescribed turbulent eddy diffusivity and $\Delta C(z)\big/\Delta z$ is the concentration gradient. Within and immediately above the canopy, $K(z)$ is parameterized as a function of friction velocity (u^*) with a small correction to account for "near-field" effects of individual canopy elements on turbulence (Raupach, 1989). In-canopy friction velocity is determined by attenuating the measured above-canopy $u*$ via an exponential function of the cumulative leaf area index (Yi, 2008). Typical values of $K(z)$ at $z/h = 0.01$ and 1 are 2.2×10^3 and $2.9 \times 10^4\,\mathrm{cm^2\,s^{-1}}$, respectively. Above $z/h = 1.25$, $K(z)$ is based on the values used by Gao et al. (1993).

Rearranging the mass balance equation (Eq. 1) shows that the vertical flux at any height, $F(z)$, is the sum of the ground-up cumulative integrals of the rate of each process:

$$F(z) = \underbrace{\int_0^z [E(z) + D(z)]dz}_{\text{Surface}} + \underbrace{\int_0^z \left[P(z) + L(z) + A(z) - \partial C(z)\big/\partial t\right]dz}_{\text{Chemical}} \quad (4)$$

As in our earlier study (Wolfe et al., 2011), we group contributions into "surface" (emission and deposition) and "chemical" (production, loss, entrainment and storage) processes. For ozone, $E(z) = 0$ and the last two chemical terms (advection and storage) are small compared to production and loss for our model conditions. Calculation of fluxes by this method yields the same values as those computed via Eq. (2). Division of each flux component by the ozone mixing ratio gives the relative contribution to the exchange velocity, which we designate as V_d and V_c for depositional and chemical velocities, respectively.

2.2 Base simulation

CAFE is currently optimized to simulate observations from BEARPEX-2007, an intensive atmospheric chemistry campaign carried out within and above a managed Ponderosa pine plantation. The site is on land owned by Sierra Pacific Industries, adjacent to the University of California's Blodgett Forest Research Station (BFRS) in the western foothills of the Sierra Nevada Mountains, CA (38°58′42.9″ N, 120°57′57.9″ W, elevation 1315 m) and has been described in detail elsewhere (Goldstein et al., 2000). The canopy consists of an overstory dominated by Ponderosa pine (height = 10 m, LAI = $3.2\,\mathrm{m^2\,m^{-2}}$) and an overstory of Ceanothus and Manzanita shrubs (heigh = 2 m, LAI = $1.9\,\mathrm{m^2\,m^{-2}}$), both of which are vertically resolved in CAFE. Meteorology and initial chemical concentrations for all model runs in this study are taken from the "hot period" discussed in Wolfe et al. (2011), which is constrained with mean noontime (11:30–12:30 PST) observations from a 7-day period (28 August–3 September, or day of year 240–246). This period was hot (27–30 °C) and dry, with relatively high concentrations of

BVOC, HO_x, ozone and oxygenated hydrocarbons and relatively low mixing ratios of NO_2 and peroxyacetyl nitrate (PAN). Average surface ozone concentrations are ∼51 ppbv for this period.

Attaining model-measurement agreement during this period requires us to implement an "enhanced OH recycling" mechanism, wherein six reactions are added to more rapidly cycle certain key organic peroxy radicals (RO_2) to OH (Wolfe et al., 2011):

$$RO_2 + HO_2 \xrightarrow{k_{rec}} \alpha OH + \text{products} \quad (5)$$

These reactions are implemented only for first-generation RO_2 derived from isoprene and 2-methyl-3-butene-2-ol (MBO), and the "products" are those derived from decomposition of the corresponding alkoxy radicals. The rate constant ($k_{rec} = 4.5 \times 10^{-11}$ cm^3 molecule^{-1} s^{-1}) and OH yield ($\alpha = 2.6$) have been tuned to optimize agreement with measured OH and HO_2 concentrations. This mechanism is a hypothesized fix to the base model OH source, which is otherwise a factor of six too small compared to observations, though we caution that it may not reflect the actual chemistry underlying the observed HO_x abundance and partitioning (Wolfe et al., 2011). We will explore the extent to which OH production from ozonolysis of reactive BVOC could provide an alternative source of OH.

In the default CAFE framework, deposition rates for both stomatal and non-stomatal uptake are calculated using a standard resistance parameterization (Wesely, 1989; Zhang et al., 2003). For BEARPEX-2007, CAFE incorporates minor adjustments to the stomatal algorithm so that modeled stomatal conductances match those derived from micrometeorological observations; however, similar independent checks on the validity of default non-stomatal resistances (cuticular and ground) are lacking. Calculation of non-stomatal deposition rates from a bottom-up approach is problematic, as this requires knowledge of both the heterogeneous loss rates and the effective molecular surface area of the canopy (Cape et al., 2009). In CAFE, non-stomatal resistances are taken from a large-scale "big leaf" model that uses a single set of parameters for a wide range of ecosystems (in this case, evergreen needle-leaf trees). These non-stomatal resistances are empirically derived from above-canopy ozone fluxes without regard for other flux-driving processes such as in-canopy BVOC chemistry (Zhang et al., 2002). It is likely that the default resistances for cuticular and ground deposition of ozone are too low and that non-stomatal deposition to surfaces is thus overestimated. For our base simulation, we set these resistances high (10^{14} s cm^{-1}) to effectively shut off non-stomatal deposition. In so doing, we attain an upper limit for the magnitude and consequences of chemical ozone fluxes. We will address how non-stomatal deposition might influence the magnitude of the chemical ozone flux inferred from observations.

2.3 VRVOC emissions and chemistry

Observed in-canopy ozone reactivity, determined from the measured suite of BVOC and known or estimated reaction rate constants, cannot explain the magnitude of inferred chemical ozone fluxes at BFRS (Goldstein et al., 2004; Bouvier-Brown et al., 2009b; Wolfe et al., 2011). For our sensitivity analysis, we add emissions and oxidation of a generic very reactive VOC (VRVOC), which is meant as a proxy for postulated but as yet undetected reactive VOC (Holzinger et al., 2005). We assume these putative VRVOC are unsaturated, cyclic terpenoid hydrocarbons. We employ a VRVOC vertical emission profile and a temperature-dependent emission rate that mimic those of the sesquiterpene class, which are among the most reactive VOC observed in this forest. The vertically-resolved emission rate takes the standard form

$$E(z) = E_b e^{\beta(T(z)-30\,^\circ\mathrm{C})} \quad (6)$$

Here, $T(z)$ is air temperature, E_b is the basal emission rate and β is the temperature coefficient. The latter two parameters are technically a function of vegetation type; for sesquiterpenes, nominal values of E_b and β for the overstory/understory are 0.4/0.16 µgC g(leaf)$^{-1}$ h^{-1} and 0.11/0.04 °C^{-1}, respectively (Bouvier-Brown et al., 2009b). The VRVOC emission rate is a tunable parameter, determined by multiplying the sesquiterpene emission rate by a constant. After accounting for canopy structure (Wolfe and Thornton, 2011), the bulk VRVOC emission flux from the canopy is distributed 56 %/44 % between the overstory/understory.

VRVOC reactions include both initial oxidation and secondary radical chemistry (Table 1). Rate constants for reactions of VRVOC with OH, O_3 and nitrate radical (NO_3) are assumed equivalent to those of β-caryophyllene, which is among the most reactive terpenoids observed at BFRS (Bouvier-Brown et al., 2009a, b). Under this assumption, the lifetimes of VRVOC against oxidation by O_3, OH and NO_3 for hot period conditions are 1.3 min, 12 min and 2700 min, respectively. This assumption of preferential oxidation by ozone is based on the requirement that these compounds induce a gradient in the ozone chemical loss rate and on the fact that CAFE accurately reproduces the measured OH reactivity during the hot period without incorporating the postulated VRVOC reactions (Wolfe et al., 2011). We will revisit our choice for these rate constants in our discussion, as they directly impact the magnitude of VRVOC emissions inferred from the model analysis.

Oxidation of VRVOC by OH and NO_3 quantitatively produces a generic peroxy radical, VRO_2. Technically, the RO_2 produced from NO_3 attack can regenerate NO_2 or form alkyl nitrates during secondary chemistry (Perring et al., 2009; Rollins et al., 2009), but we neglect this detail since modeled daytime NO_3 mixing ratios are too small (∼10^5 molecules cm^{-3}) under our conditions to affect the

Table 1. Chemical reactions for VRVOC. Rate constants for initial oxidation reactions are the same as those used for β-caryophyllene (Bouvier-Brown et al., 2009b; Wolfe and Thornton, 2011). The yield of OH and VRO_2 from VRVOC ozonolysis (y) is taken as an adjustable constant ranging from 0 to 1. Rate constants and product yields for reactions of peroxy radicals (VRO_2) are the same as those for β-pinene RO_2.

Reaction	$k/\mathrm{cm^3\,molec^{-1}\,s^{-1}}$
$\mathrm{VRVOC + OH \rightarrow VRO_2}$	2.0×10^{-10}
$\mathrm{VRVOC + O_3 \rightarrow}\ y\mathrm{OH} + y\mathrm{VRO_2} + (1-y)\mathrm{VROX}$	1.2×10^{-14}
$\mathrm{VRVOC + NO_3 \rightarrow VRO_2}$	2.2×10^{-11}
$\mathrm{VRO_2 + NO \rightarrow VROX + NO_2 + HO_2}$	$2.54\times10^{-12}\exp(360/T)$
$\mathrm{VRO_2 + HO_2 \rightarrow VROX}$	$0.914\left[2.91\times10^{-13}\exp(1300/T)\right]$
$\mathrm{VRO_2 + RO_2 \rightarrow VROX + 0.7\,HO_2}$	9.0×10^{-14}

main conclusions presented herein. Reactions of VRO_2 with NO, HO_2 and RO_2 are treated analogously to those of the generic sesquiterpene and monoterpene-derived RO_2 radicals in CAFE (Wolfe and Thornton, 2011). These VRO_2 reactions all produce VROX, which is a generic species representing closed-shell oxidation products. In our sensitivity simulations we will explore the possible fates of VROX, which might undergo further oxidative chemistry, deposit to canopy surfaces or partition to aerosol.

VRVOC ozonolysis is slightly more complex than oxidation by OH or NO_3. Reaction of ozone with alkenes typically proceeds via addition to the double-bond followed by rapid decomposition into a thermally-excited Criegee biradical and a closed-shell ketone or aldehyde (for ring-breaking reactions, the biradical and closed-shell oxy-moeity remain on a single molecular backbone). The short-lived Criegee intermediates decompose via several pathways, including collisonal stabilization, isomerization to a highly-energized hydroperoxide, or rearrangement to a highly-energized ester; these products may undergo further prompt isomerization/decomposition reactions (Atkinson and Arey, 2003). OH and RO_2 yields from ozonolysis depend on the specific structure of the precursor VOC; for example, first-generation RO_2 yields from the ozonolysis of α-pinene and β-pinene are 0.8 and 0.3, respectively (Atkinson and Arey, 2003). Within the accepted mechanism, OH and RO_2 mainly derive from hot hydroperoxide decomposition channels and are always produced together. With these considerations in mind, we implement the ozonolysis reaction as

$$\mathrm{VRVOC + O_3 \rightarrow}\ y\mathrm{OH} + y\mathrm{VRO_2} + (1-y)\mathrm{VROX} \quad (7)$$

where y is a tunable yield ranging from 0 to 1. Our sensitivity analysis includes an examination of how the value of y impacts canopy oxidant chemistry. We choose the maximum VROX yield to be 1 so that the VROX mixing ratio remains representative of the total amount of VRVOC processed. In other words, we do not account for the production of multiple closed-shell oxidized VOC from a single ozonolysis reaction. In all simulations, concentrations of VRVOC, VROX and VRO_2 are initialized to 1 molecule $\mathrm{cm^{-3}}$.

2.4 Overview of sensitivity simulations

Here we summarize the general methodology for the sensitivity experiments; details for specific model scenarios may be found in Table 2 and throughout Sect. 3. Starting from the base simulation, in which VRVOC concentrations and emission rates are zero, we first implement VRVOC emissions with a basal emission rate chosen to optimize model-measurement agreement of ozone exchange velocities. For this model run, OH yields from VRVOC ozonolysis are set to zero ($y = 0$), and VROX is treated as a stable end-product that does not react or deposit but does undergo vertical mixing. We refer to this case as the high reactivity (HR) scenario.

Subsequent simulations involve modifications to the HR scenario to probe the potential impacts of VRVOC chemistry on forest-atmosphere ozone exchange and in-canopy photochemistry. First, we examine the sensitivity of the chemical ozone flux to the canopy mixing timescale and temperature and discuss how our choices for non-stomatal deposition and the $\mathrm{VRVOC + O_3}$ reaction rate constant influence model results. Next, we vary the OH yield from VRVOC ozonolysis to characterize perturbations to radical chemistry and partitioning. We conclude with a discussion on the nature and fate of the VROX oxidation products. These compounds may deposit to canopy surfaces, undergo further chemical reactions or contribute to organic aerosol mass, and we investigate each of these possibilities in turn.

3 Results and discussion

3.1 Base scenario

Figure 1 summarizes the primary contributors to chemical production and loss of ozone as modeled with the default CAFE chemical mechanism. In this case, reactions between

Table 2. Summary of sensitivity simulations. Specific details for individual model runs can be found in the appropriate sections of the text.

Scenario	Parameter(s) adjusted	Values	Section Discussed
Base	–	–	3.1
NS deposition	Non-stomatal (cuticular + ground) O_3 deposition velocity	$-0.15\,cm\,s^{-1}$	3.3
High reactivity	VRVOC emission flux	$30\,\mu mol\,m^{-2}\,h^{-1}$	3.2
Diffusion sensitivity[a]	Canopy mixing time (τ)[b]	2[c], 4, 6, 8, 10 min	3.4
Temperature sensitivity[a]	Average in-canopy air temperature	10, 15, 20, 25, 30[c] °C	3.4
Ozonolysis OH source[a]	OH yield (y) from VRVOC + O_3	0[c], 0.2, 0.75[d]	3.5
VROX deposition[a]	VROX deposition velocity	0[c], −0.7, −1.4, −2.1, −2.8, $-3.5\,cm\,s^{-1}$	3.6.1
VROX ozonolysis[a]	VROX + O_3 rate constant	0[c], 1.2, 3.6, 6.0×10^{-15} $cm^3\,molec^{-1}\,s^{-1}$	3.6.3

[a] Also includes high VRVOC reactivity.
[b] Adjusted by uniformly decreasing in-canopy diffusion coefficient, $K(z)$.
[c] Starting value for base and high reactivity scenarios.
[d] For this model run, enhanced OH recycling was not implemented.

ozone and the nitrogen oxides ($NO + NO_2 = NO_x$) dominate gross ozone chemistry:

$$NO_2 + h\nu \rightarrow NO + O(^3P) \quad (8)$$

$$O(^3P) + O_2 \rightarrow O_3 \quad (9)$$

$$NO + O_3 \rightarrow NO_2 + O_2 \quad (10)$$

Below $z/h = 0.35$ (3.5 m), the net effect of Reactions (8–10) is destruction of ozone, while above this height NO_x chemistry yields net production of ozone. This behavior is related to the interplay of soil NO emissions, radiation extinction, vertical mixing and chemistry (Dorsey et al., 2004; Duyzer et al., 2004; Gao et al., 1993; Walton et al., 1997; Wolfe et al., 2011). Net production above the canopy is likely due to reactions of soil-emitted NO with HO_2 and RO_2 radicals. Other reactions contributing to ozone chemistry are markedly slower and include net destruction by photolysis and reactions with BVOCs:

$$O_3 + h\nu \rightarrow O(^1D) + O_2 \quad (11)$$

$$O(^1D) + H_2O \rightarrow 2OH \quad (12)$$

$$O(^1D) \xrightarrow{N_2,O_2} O(^3P) \quad (13)$$

$$O_3 + BVOC \rightarrow products \quad (14)$$

Photolysis is a net loss of ozone only when the product, $O(^1D)$, reacts with water vapor to form OH. Primary BVOC sinks for ozone include sesquiterpenes (SQT), monoterpenes (MT), 2-methyl-3-buten-2-ol (MBO) and isoprene. Modeled concentrations of NO_2 and VOC agree reasonably well with observations from this period, as detailed in Wolfe et al. (2011).

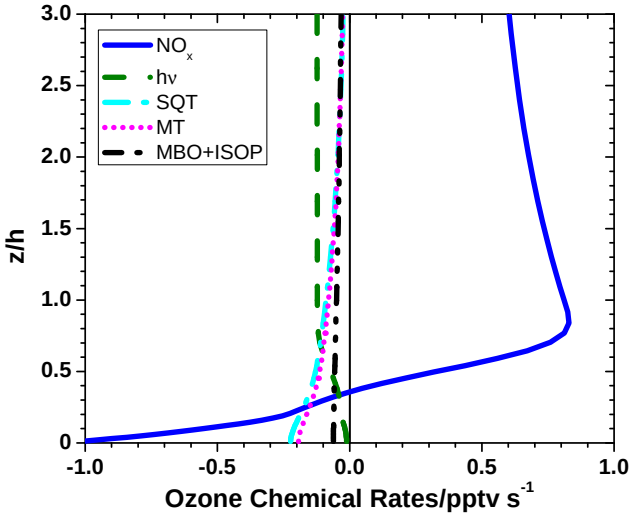

Fig. 1. Vertical profile of contributions to chemical production and loss of ozone for the base scenario. The "NO_x" profile represents the sum of rates for the $NO + O_3$ reaction and NO_2 photolysis. The "$h\nu$" profile represents the net loss of ozone from photolysis after accounting for the branching of $O(^1D)$ reactions between quenching and reaction with water vapor.

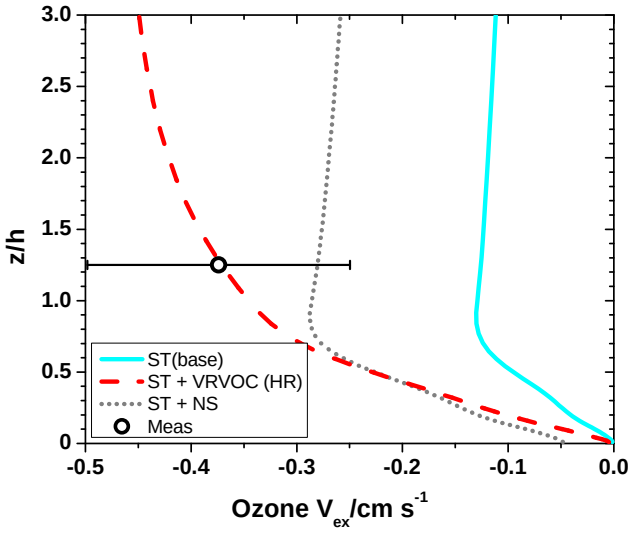

Fig. 2. Vertical profiles of modeled ozone exchange velocity for the base scenario (stomatal deposition only), the HR scenario (stomatal deposition and VRVOC reactions) and a model scenario using default resistances for non-stomatal deposition. The measured value (mean $\pm 1\sigma$) is also shown.

Following Eq. (4), the contribution of each of these terms to the chemical ozone flux at any height z is

$$F_c(z) = \int_0^z \left(\frac{d[O_3](z)}{dt}\right) dz \quad (15)$$

where the integrand represents the net rate of change of ozone for a given reaction or set of reactions. Integrating from the ground to $z/h = 1.25$ (12.5 m, the height of most previous ozone flux measurements at BFRS), the chemical ozone fluxes due to NO_x, photolysis and known BVOC reactions are 0.81, -0.29 and -0.48 µmol m^{-2} h^{-1}, respectively. Despite the relatively large rates for NO_x-O_3 chemistry, the flux of ozone due to this chemistry is of the same magnitude as those for photolysis and BVOC reactions because loss in the lower canopy partly cancels production above when taking the integral. The NO_x-driven flux is modestly sensitive to the prescribed soil NO emission rate; for example, doubling the soil NO flux from 3 to 6 ngN m^{-2} s^{-1} leads to a 25 % increase in net ozone production at $z/h = 1.25$. In total, known chemistry imparts a slight positive component of 0.04 µmol m^{-2} h^{-1} to the ozone flux at this height. For comparison, the chemical ozone flux estimated from previous observations at BFRS is on the order of -20 µmol m^{-2} h^{-1} (Kurpius and Goldstein, 2003). This flux is 42 times higher than the modeled flux from reactions with known BVOC.

As shown in Fig. 2, the average observed noontime ozone exchange velocity for the hot period is -0.37 ± 0.12 cm s^{-1} (mean $\pm 1\sigma$). For an average ozone mixing ratio of 51 ppbv, this corresponds to an ozone flux of -24 µmol m^{-2} h^{-1}. In our base scenario, stomatal deposition imparts an above-canopy deposition velocity of -0.13 cm s^{-1} and accounts for ~33 % of the observed forest-atmosphere exchange, consistent with previous analyses of summertime ozone fluxes at BFRS (Fares et al., 2010a; Goldstein et al., 2004; Kurpius and Goldstein, 2003). Thus, we estimate a non-stomatal ozone flux of -16 µmol m^{-2} h^{-1} for our conditions.

3.2 High reactivity scenario

In going from the base to the HR scenario, we implement the VRVOC chemical mechanism described in Sect. 2.3 and set the VRVOC basal emission rates so that the resulting chemistry drives the entire non-stomatal component (67 %) of the ozone flux (Fig. 2). For our particular conditions, this stipulation requires a VRVOC emission flux of 30 µmol m^{-2} h^{-1}, which is 36 times the modeled SQT emission flux. The corresponding basal emission rates (e.g. at 30 °C) for the overstory and understory are 1.3×10^{13} and 0.6×10^{13} molecules per gram of leaf per second, respectively. Assuming the hydrocarbons represented by VRVOC contain 10–15 carbons per molecule, the resulting carbon-weighted emission flux of 3.5–5.4 mgC m^{-2} h^{-1} is 1.4–2.1 % of the observed noontime CO_2 uptake for this period. For comparison, the carbon flux associated with known BVOC (primarily 2-methyl-3-buten-2-ol, methyl chavicol, MT and SQT) is estimated to be 1.8–12 % of the annual net ecosystem exchange at this forest (Bouvier-Brown et al., 2011). Our model results for highly-reactive BVOC emission fluxes agree well with previous canopy-integrated estimates of 13–66 µmol m^{-2} h^{-1} derived from observations at this forest (Table 3).

Consistent with the prescribed reactivity, VRVOC are rapidly oxidized in the canopy air space. The average VRVOC loss rate below $z/h = 1.25$ is -2.1×10^8 molecules cm^{-3} s^{-1}, where reaction with ozone accounts for ~95 % of this loss. OH reaction contributes the remaining 5 %, while reaction with NO_3 in this canopy is negligibly slow (~10^5 molecules cm^{-3} s^{-1}). For comparison, Holzinger et al. (2005) infer a missing BVOC "reactivity" of 1.8–8.8 $\times 10^8$ molecules cm^{-3} s^{-1} based on observations of oxidized VOC at BFRS in 2003 (Table 3). The resulting VRVOC chemical lifetime of less than 80 seconds leads to a VRVOC escape efficiency – defined as the ratio of the net canopy-top flux to the canopy-integrated emission flux – of 0.5. In other words, 50 % of emitted VRVOC is consumed within the canopy airspace. This value is somewhat higher than the β-caryophyllene escape efficiency of 0.30 estimated by a similar model for a different forest (Stroud et al., 2005), though we note that the modeled escape efficiency depends on several prescribed variables, including VRVOC reaction rate coefficients, canopy mixing timescales and the distribution of VRVOC emissions between the overstory and understory. Given our modeled escape efficiency, VRVOC mixing ratios averaged over the canopy are 40 times higher than the boundary layer (800 m) average. In contrast, VROX mixing ratios averaged over the canopy are only twice the boundary layer average

Table 3. Comparison of model results from the high reactivity (HR) scenario with previous observationally-constrained estimates.

Quantity	This study	Previous work	Units	Reference[a]
VRVOC emission flux	30	13–66[b]	$\mu mol\,m^{-2}\,h^{-1}$	i
Carbon emission	1.4–2.1[c]	0.5–2.4[d]	% of CO_2 flux	i
VRVOC loss rate	2.0 (O_3) 0.1 (OH)	1.8–8.8[e]	10^8 molecules $cm^{-3}\,s^{-1}$	i
Non-stomatal component of ozone flux	67	43–70	% of total O_3 flux	ii, iii
Ozone chemical flux	−16	−20	$\mu mol\,m^{-2}\,h^{-1}$	iii
Ozone chemical velocity	−0.25	−0.3[f]	$cm\,s^{-1}$	iii

[a] (i) Holzinger et al. (2005). (ii) Fares et al. (2010a). (iii) Kurpius and Goldstein (2003).
[b] VRVOC emissions inferred by assuming a 10–50 % yield of measured oxidation products.
[c] Assuming VRVOC contains 10–15 carbons.
[d] Assuming VRVOC contains 10 carbons.
[e] Total reaction rate, scaled to the ozone flux measurement height of 12.5 m.
[f] For an average ozone mixing ratio of 55 ppbv.

when VROX sinks are not included. Thus, the impact of compounds within the VRVOC class is likely limited to local photochemistry within and just above the canopy, while their oxidation products – depending on their lifetimes – could have a more regional influence.

The presence of VRVOC only slightly perturbs modeled ozone abundance (∼6 % decrease) but strongly alters the vertical profile of the ozone exchange velocity. The vertical profile of the ozone exchange velocity (Fig. 2) is more pronounced above $z/h = 0.7$ in the HR scenario than in the deposition-only case because the chemical ozone sink is extended out of the canopy by vertical mixing. An opportunity for experimentally testing the chemical flux hypothesis thus arises given that the shape of the exchange velocity gradient is indicative of the relative contributions of mobile (e.g. chemical) and immobile (e.g. depositional) drivers of surface exchange. For BFRS conditions, the difference in exchange velocities between any two reasonable observation heights might be difficult to discern with state-of-the-art eddy covariance techniques; for example, the ozone exchange velocity changes by 30 % between $z/h = 1$ and 3. For a taller forest with stronger BVOC emissions and a longer transport timescale through the surface layer, however, flux divergence measurements might provide a useful tool to assess the nature of the dominant near-surface sources or sinks.

Following Eqs. (3) and (15), the component of the ozone exchange velocity at the measurement height (z_m) due to in-canopy reactions with VRVOC having rate constant k is given by

$$V_c(z_m) = \frac{\int_0^{z_m} -k[\mathrm{VRVOC}][\mathrm{O_3}]dz}{[\mathrm{O_3}]_{z_m}} \cong -\int_0^{z_m} k[\mathrm{VRVOC}]dz \quad (16)$$

In the present study, we choose to generate the desired chemical ozone flux by adjusting the VRVOC emission flux; however, we could instead prescribe VRVOC emissions and tune the rate constant (k) to arrive at the same flux. Thus, we have effectively constrained the in-canopy loss rate of ozone to VRVOC (hereafter referred to as VRVOC reactivity), which is a function of the product of the rate constant and the VRVOC concentration. If the rate constant for reaction of VRVOC with ozone were set higher or lower, we would require proportionally less or more VRVOC emissions to attain agreement with observed ozone fluxes. Thus, any estimates derived from the VRVOC emission flux, such as the carbon efflux ascribed to these unidentified hydrocarbons (Table 3), will depend on this rate constant. The chosen value of $1.2 \times 10^{-14}\,cm^3\,molec^{-1}\,s^{-1}$ is the same as that for reaction of ozone with β-caryophyllene, which is the most reactive sesquiterpene observed at BFRS. The only well-known BVOC that is more reactive to ozone is α-terpinene, a monoterpene with an ozone reaction rate constant of $2.1 \times 10^{-14}\,cm^3\,molec^{-1}\,s^{-1}$ (Calogirou et al., 1999). Downstream chemistry, including VROX production and perturbations to RO_x abundance and partitioning, is essentially independent of our choice for this rate constant. These aspects of our model results (discussed below) depend only on the total VRVOC reactivity, which is constrained by the difference between the observed ozone exchange velocity and the observationally-derived stomatal conductance.

The chemical influence on ozone fluxes is quite evident in the modeling results from the HR scenario even though the average lifetime of ozone against loss to VRVOC in the model is 65 min within the canopy – much longer than the canopy residence time of ∼2 min. Thus, comparing such timescales (e.g. calculation of a "Damköhler number", $Da = \tau_{mix}/\tau_{chem}$) may not be an appropriate metric for assessing the potential chemical perturbation to forest-atmosphere exchange of reactive species. We have also demonstrated this point for acyl peroxy nitrates (Wolfe et al., 2011). These examples involve chemistry-induced losses driving downward fluxes; however, it is reasonable that relatively slow but sustained net in-canopy production could

also induce an efflux of these and other chemical species. Detailed resolved-canopy modeling of flux observations thus remains an important tool to assess these various pathways.

3.3 Role of non-stomatal deposition

The challenges of correctly partitioning ozone fluxes become apparent when considering the implications of uncertainties in non-stomatal deposition. At the outset of our assessment of the ozone flux budget, we neglected non-stomatal deposition pathways to simplify our analysis and maintain a focus on the potential effects of a chemical ozone flux. If we had instead used the default CAFE resistances for cuticular and ground deposition (based on typical literature values), the modeled ozone exchange velocity without VRVOC would be low by 25 % relative to the mean but within the range of observations (Fig. 2). In this case, even though the need for chemical fluxes becomes questionable in light of the observational spread and other uncertainties (e.g. turbulent transport), the VRVOC emission flux required to make up the 25 % difference between measured and modeled mean values would still be a factor of 14 larger than the SQT emission flux in the base CAFE model. In other words, relatively small errors in non-stomatal deposition rates of ozone have large consequences for the implied presence of VRVOC.

As noted in Sect. 2, non-stomatal resistance parameterizations are not well-constrained by independent measurements and are thus highly uncertain. A recent inter-comparison of large-scale dry deposition models used by US and Canadian environmental agencies identified differences in the parameterization of cuticular and ground deposition as a major source of discrepancy between the two models (Schwede et al., 2011). To some extent, these issues stem from the fact that the underlying mechanisms of surface loss are not well understood. Cape et al. (2009) suggest that decomposition of ozone to molecular oxygen on canopy surfaces can account for an ozone deposition velocity of as much as a few mm s^{-1}, though the magnitude of this number will vary greatly between forests and there are too few laboratory studies on actual vegetation to develop a viable parameterization. Leaf and branch-level enclosure experiments have reported negligible cuticular ozone deposition to Loblolly pine (Karl et al., 2005) and citrus trees (Fares et al., 2010b). It could thus be argued that non-stomatal ozone deposition parameterizations have been developed to explain non-stomatal fluxes caused by an entirely different process: homogeneous gas-phase chemistry, not surface deposition. Given these uncertainties, we will neglect this process for the remainder of our study with the inherent caveat that non-stomatal ozone deposition would decrease the amount of VRVOC reactivity invoked from comparison of modeled and measured ozone fluxes.

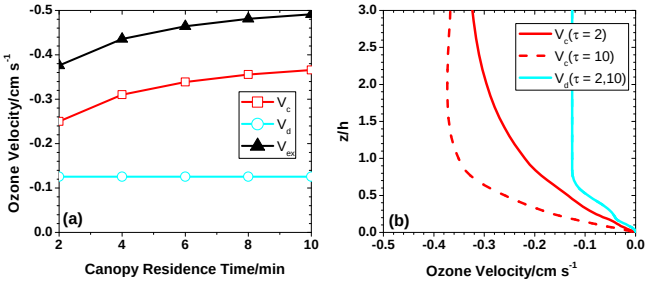

Fig. 3. (a) Influence of canopy residence time on modeled chemical velocity (V_c), stomatal deposition velocity (V_d) and total exchange velocity (V_{ex}) for ozone at $z/h = 1.25$. **(b)** Vertical profiles of the ozone chemical and stomatal deposition velocity for canopy residence times of 2 and 10 min.

3.4 Sensitivity to vertical transport and temperature

Due to its dependence on in-canopy VRVOC concentrations, the magnitude of the chemical ozone flux should be sensitive to vertical mixing within the canopy airspace. To assess this effect, we performed a series of model runs where the in-canopy eddy diffusivity (K) was uniformly decreased throughout the canopy to produce canopy residence times of 2 to 10 min. The canopy residence time (τ) can be estimated as the sum of the "aerodynamic resistances" (R_a) within each model layer (Baldocchi, 1988):

$$\tau = h\sum_{i=1}^{36}\frac{\Delta z_i}{K(z_i)} = h\sum_{i=1}^{36}R_{a,i} \quad (17)$$

The lower limit of 2 min represents our HR scenario and is essentially the smallest mixing time attainable for the prescribed friction velocity profile (Wolfe and Thornton, 2011). This value is also close to the canopy mixing time of 1.5 min estimated by Holzinger et al. (2005) via observations of sweep-ejection events. The upper limit of 10 min is close to the wintertime value for BFRS estimated from HNO_3 flux observations (Farmer and Cohen, 2008).

Figure 3a shows the resulting model trends in chemical velocity (V_c), stomatal deposition velocity (V_d) and total exchange velocity (V_{ex}) for ozone at $z/h = 1.25$. The chemical velocity increases by 46 % between $\tau = 2$ and 10 min. The chemical velocity does not scale 1:1 with canopy residence time in the model because decreased eddy diffusivity partly offsets the steeper ozone concentration gradient in the determination of the modeled ozone flux (Eq. 2). The gradient of V_c (Fig. 3b) becomes steeper in the canopy but more vertical above, suggesting that VRVOC reactivity is increasingly confined to the canopy airspace and consistent with a decrease in the VRVOC escape efficiency from 0.5 at $\tau = 2$ min to 0.24 at $\tau = 10$ min. In contrast, the deposition velocity is unaffected. As highlighted in our earlier discussion of the ozone flux divergence (Sect. 3.2), this behavior is a consequence of the nature of these sinks. The

chemical velocity of ozone is sensitive to VRVOC concentrations, which are 46 % higher in the canopy when the residence time is 10 min. Thus, inhibition of vertical mixing leads to a greater sequestration of chemical ozone sinks within the canopy, which in turn can enhance the chemical perturbation to forest-atmosphere ozone exchange. Deposition, on the other hand, is a first-order loss process with rate constants that depend only on parameterized resistances and leaf area. Thus the deposition velocity – which is the integral of the deposition rate constants over the vertical coordinate – is essentially diffusion-independent for the range of eddy diffusivities probed here. Ozone deposition via stomatal uptake might be slightly reduced if decreased diffusion is accompanied by decreased friction velocities, which would result in a larger laminar sublayer resistance; however, as the stomatal resistance is typically the limiting factor at this forest, such effects should be minor.

Previous inferences of chemical ozone fluxes have relied partly on the temperature dependence of the non-stomatal component, which can mimic the exponential profile of terpene emissions (Kurpius and Goldstein, 2003). Figure 4a summarizes results from a series of model runs where we decreased the prescribed temperature profile to give average in-canopy air temperatures of 30, 25, 20, 15 and 10 °C. The 30 °C point represents the HR scenario. Consistent with our parameterized VRVOC temperature dependence (Eq. 6), the chemical velocity changes by a factor of 5 over this range of temperatures. Conversely, the stomatal deposition velocity increases by a factor of 2 owing to an accompanying drop in the model-calculated vapor pressure deficit that reduces the stomatal resistance. Unlike in the case of changing vertical diffusion, vertical profiles of V_c and V_d maintain the same relative gradient with changing temperature (Fig. 4b). The temperature-sensitive partitioning of modeled ozone fluxes between chemistry and stomatal uptake leads to a modest decrease of ∼22 % in the total ozone exchange velocity. According to our model results, chemical ozone fluxes would dominate the ozone flux budget above 26 °C in the absence of non-stomatal deposition. This result is consistent with Kurpius and Goldstein (2003), who showed that deposition is the dominant driver for ozone fluxes in all seasons except summer – when BVOC emissions are highest.

3.5 RO_x chemistry

The addition of VRVOC chemistry – even without OH production from ozonolysis – appreciably alters modeled RO_x ($RO_x = OH + HO_2 + RO_2$) profiles (Fig. 5). Note that profiles of OH and HO_2 for the base scenario are constrained by observations at $z/h = 0.99$ and 1.5 (Wolfe et al., 2011). The RO_2 mixing ratio, which represent the steady-state sum of 155 organic peroxy radicals, is not constrained by observations but has been shown to be consistent with previous steady-state estimates for this forest (LaFranchi et al., 2009). OH, HO_2 and total RO_2 concentrations respectively decrease by 25–

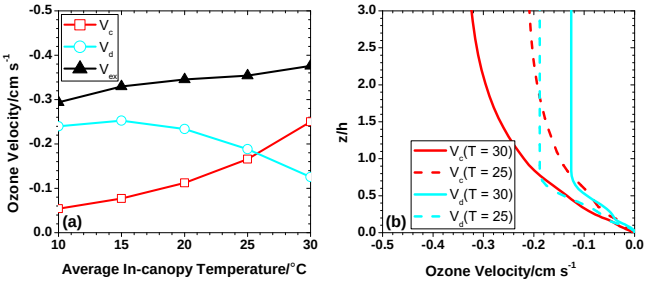

Fig. 4. **(a)** Influence of air temperature on modeled chemical velocity (V_c), stomatal deposition velocity (V_d) and total exchange velocity (V_{ex}) for ozone at $z/h = 1.25$. **(b)** Vertical profiles of the ozone chemical and stomatal deposition velocity for average in-canopy temperatures of 30 °C and 25 °C.

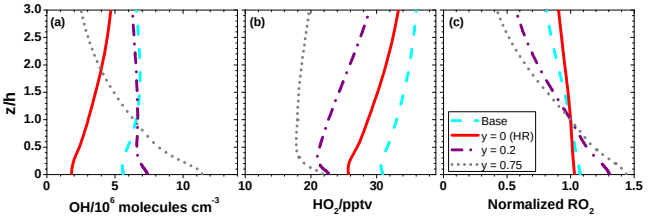

Fig. 5. Vertical profiles of OH **(a)**, HO_2 **(b)** and RO_2 **(c)** for the OH-yield sensitivity scenarios as described in the text. RO_2 concentrations are normalized to canopy-top values of 129, 101, 268 and 564 pptv for the base, HR, $y = 0.2$ and $y = 0.75$ scenarios, respectively. Note that the $y = 0.75$ case does not include an enhanced OH recycling mechanism.

75 %, 17 % and 23 % in the HR scenario. These changes reflect the reaction between VRVOC and OH, which channels OH into VRO_2 at the expense of other RO_2-forming reactions. Specifically, less OH is available to form the MBO and isoprene-derived RO_2 that participate in our enhanced recycling mechanism, which then feeds back into total OH production. The OH gradient also becomes steeper in the HR scenario, with lower concentrations near the ground where VRVOC concentrations are highest. We caution that the magnitude of changes in RO_x abundance is somewhat arbitrary, as it depends on the choice for the rate constant of the reaction between VRVOC and OH, as well as on the OH yield from VRVOC ozonolysis.

As discussed in detail in the original CAFE evaluation study (Wolfe et al., 2011), the default MCM chemical mechanism under-predicts measured OH concentrations by a factor of six for the conditions of our base scenario. We therefore incorporate a mechanism that effectively forces primary RO_2 from isoprene and MBO into OH (Eq. 5). This scheme may not accurately represent the actual chemistry controlling the RO_x budget at this location. In our previous study, we neglected VRVOC ozonolysis reactions as a source of OH in and above the canopy. Such "dark" OH sources have been implicated in observations of anomalously high nighttime

OH mixing ratios in other forests (Faloona et al., 2001) and could also be important during the day (Tan et al., 2001). OH yields from reaction of ozone with biogenic alkenes depend on the specific structure of the BVOC precursors, ranging from 0.06 for β-caryophyllene to near-unity for terpenes with tri- and tetra-substituted C=C bonds (Aschmann et al., 2002; Atkinson and Arey, 2003; Shu and Atkinson, 1994). Previous estimates for BFRS advocate an OH production rate of 1.5 to 3×10^8 molecules cm^{-3} s^{-1} from VRVOC ozonolysis (Goldstein et al., 2004), while our model analysis of OH mixing ratios measured during BEARPEX 2007 at $z/h = 0.99$ (9.9 m) using the base MCM v3.1 suggests that an additional OH production source of 0.7×10^8 molecules cm^{-3} s^{-1} is needed to close the OH budget (Wolfe et al., 2011).

Starting from the model setup for the HR scenario, we perform two additional model runs where we vary the OH yield from VRVOC ozonolysis (Table 1) from $y = 0$ to $y = 0.2$ and $y = 0.75$. The first scenario ($y = 0.2$) retains enhanced OH recycling from primary isoprene and MBO RO_2, as in the base and HR cases. In the second scenario, recycling reactions are neglected entirely, as an ozonolysis OH yield of $y = 0.75$ is sufficient to match observed OH concentrations at $z/h = 0.99$ without invoking additional chemistry. At higher OH yields from VRVOC ozonolysis, the in-canopy OH gradient shifts from increasing to decreasing with height (Fig. 5a). The OH profile in the most extreme case ($y = 0.75$) mirrors the VRVOC concentration gradient. Absolute HO_2 concentrations decrease by ~30 % (Fig. 5b) in the $y = 0.75$ case, while HO_2 vertical gradients become enhanced near the ground. These changes reflect the increasing importance of VRO_2 for HO_2 chemistry, which acts as both a sink via direct reaction and as a source through the reaction of VRO_2 with NO.

As OH is always produced alongside a peroxy radical in the standard ozonolysis mechanism (Sect. 2.3), the parameter y also represents the yield of VRO_2 (Table 1). For the $y = 0.75$ scenario, total RO_2 concentrations are 45 % higher at the ground than at canopy top (Fig. 5c), and VRO_2 comprises 67 % of total average RO_2 in the canopy, which has reached ~670 pptv. Mixing ratios of other RO_2 species also grow with increasing y because of a decrease in NO concentrations and, in the $y = 0.75$ case, a lack of extra RO_2 sinks that otherwise exist when employing the enhanced recycling mechanism. Even for the $y = 0.2$ scenario, total RO_2 is ~300 pptv, which is roughly a factor of two higher than both previous estimates for this forest (LaFranchi et al., 2009) and measurements at other forested locations (Cantrell et al., 1992; Qi et al., 2005). Such high RO_2 levels also impact other aspects of the chemistry. For example, canopy-averaged NO/NO_2 ratios for the base, HR, $y = 0.2$ and $y = 0.75$ scenarios are 0.18, 0.21, 0.12 and 0.07, respectively.

These sensitivity tests effectively place a limit on the production rate of OH from postulated VRVOC, which in our tests ranges from 0 for the HR scenario to 2.1 and 7.8 pptv s^{-1} in the $y = 0.2$ and $y = 0.75$ scenarios, respectively. Considering the substantial perturbation to RO_2 concentrations and concomitant impacts on HO_2 chemistry, VRVOC ozonolysis is unlikely to contribute more than ~1 pptv s^{-1} to OH production at this site. This rate corresponds to a yield of ~0.1 for the VRVOC reactivity imposed in this study. By comparison, the canopy-averaged total OH production rate in the base scenario is 3.8 pptv s^{-1}. It is possible that our simple mechanism has neglected additional sinks of VRO_2 radicals, such as unimolecular isomerization/decomposition (Glowacki and Pilling, 2010) or surface deposition, which would reduce the buildup of VRO_2 in the canopy. For example, VRO_2 concentrations decrease by 20 % when we force VRO_2 to deposit at the aerodynamic limit, though even this loss would be insufficient to bring the modeled NO/NO_2 ratio for the $y = 0.75$ case into the range expected for this forest. Ozonolysis of the oxidation products, represented by VROX, might provide an additional source of OH radicals; however, OH yields from reactions of terpene oxidation products are thought to be 2–10 times lower than those from ozonolysis of the primary hydrocarbons (Herrmann et al., 2010). Ultimately, OH yields will depend on the structure of the BVOC in question, particularly the substitution order of double bonds and the branching of Criegee intermediates. In summary, if VRVOC reactions with ozone drive a significant fraction (e.g. ~50 %) of the ozone flux, it is unlikely that these reactions are simultaneously a significant source of OH and RO_2 radicals without implying a need for drastic revision of the current accepted chemistry of such RO_2.

3.6 Fate of VRVOC oxidation products

In the HR scenario, VROX mixing ratios grow to 3.3 ppbv averaged over the canopy, or 1.6 ppbv averaged over the whole 800 m boundary layer. This "lumped" species represents a wide array of oxidized hydrocarbons, including ketones, aldehydes, alcohols and carboxylic acids, and consists of both small-chain VOCs (e.g. formaldehyde, glyoxal, formic acid, etc.) and larger oxidation products that retain some structure of the precursor species. Though we did not include VROX sinks in our initial model runs, these compounds are almost certainly subject to both physical and chemical losses. Here we explore the potential effects of such processes, with a specific focus on surface deposition, partitioning to aerosol and secondary oxidative chemistry.

3.6.1 Deposition

Recent work by Karl et al. (2010) demonstrates that oxidized VOCs, such as methyl vinyl ketone and methacrolein, can deposit readily to forest canopies. Observations of above-canopy fluxes of these compounds suggest deposition velocities of a few cm s^{-1}, which is comparable to simultaneously measured ozone exchange velocities. We should thus expect that some of the postulated compounds represented by

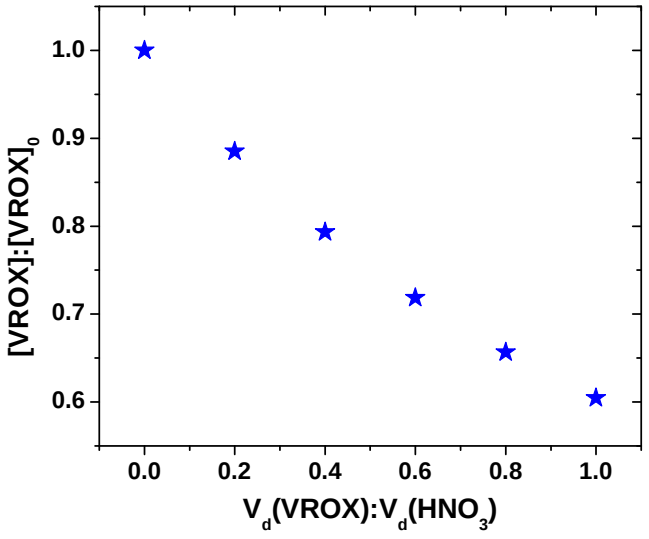

Fig. 6. Influence of deposition on modeled VROX concentrations. The VROX deposition velocity (V_d) is given as a ratio to that of nitric acid, which represents the "aerodynamic limit" for deposition. VROX concentrations represent an average over the canopy and are normalized to the concentration for the case with no deposition (3.3 ppbv).

VROX would deposit to canopy surfaces. Lower-volatility oxidation products, such as those that retain the carbon backbone and thus acquire a higher degree of functionality, may deposit even more efficiently. For highly adhesive or soluble molecules, it is often assumed that deposition occurs at the "aerodynamic limit." In such a case, every collision with the surface results in the loss of the gas-phase molecule, and the deposition rate is limited only by turbulent and molecular diffusion to the canopy elements.

Figure 6 illustrates the impact of deposition on modeled VROX concentrations. The slight curvature of this plot reflects the limiting influence of turbulent transport to the surface at higher deposition velocities. At the aerodynamic limit (equal to the deposition velocity of nitric acid, $-3.5\,\mathrm{cm\,s^{-1}}$), canopy-averaged VROX concentrations are lowered by ∼40 % relative to the case with no deposition. True deposition rates of these compounds are likely lower than in this limiting case, especially when averaged over all potential varieties of VROX. To our knowledge, however, current resistance-based deposition models typically parameterize non-stomatal surface uptake on the sole basis of aqueous solubility and reactivity (Wesely and Hicks, 2000). These models do not account for volatility, which could be a driving force for condensation of oxidized hydrocarbons onto canopy surfaces in a manner similar to gas-to-particle partitioning (Hallquist et al., 2009).

3.6.2 Aerosol uptake

Semi-volatile compounds produced during VRVOC oxidation might also partition to particles, thereby contributing to the growth of secondary organic aerosol (SOA). SOA mass yields from terpene ozonolysis typically range from 0 to 50 % (Lee et al., 2006a; Winterhalter et al., 2009), and are strongly dependent on ambient organic aerosol mass concentration. A recent study of β-caryophyllene ozonolysis suggests an SOA yield of 6 % in the presence of $50\,\mu\mathrm{g\,m^{-3}}$ of organic aerosol (Winterhalter et al., 2009), which we will take as an upper limit given the low organic aerosol mass observed at this site (see below). Combining this yield with the boundary layer average VROX mixing ratio of 1.6 ppbv and assuming a VRVOC molar mass of 136 to 204 g $\mathrm{mol^{-1}}$ (in analogy to monoteprenes and sesquiterpenes), we calculate a potential organic aerosol mass concentration of 0.5–$0.7\,\mu\mathrm{g\,m^{-3}}$ from VROX alone. For comparison, observations from BEARPEX-2007 indicate an average organic aerosol mass of $2.5 \pm 0.9\,\mu\mathrm{g\,m^{-3}}$ for our hot period (Farmer et al., 2011), which is also consistent with the PM_{10} organic matter loading of $2.1 \pm 1.2\,\mu\mathrm{g\,m^{-3}}$ estimated for this region in summer 2003 (Cahill et al., 2006). In the latter study, a speciated analysis was able to account for only 23 % of the total organic aerosol mass, implying an unidentified aerosol organic mass of $\sim 1.6\,\mu\mathrm{g\,m^{-3}}$. In-canopy VROX production, at a rate consistent with the non-stomatal component of the ozone flux, followed by ventilation to the boundary layer and subsequent gas-particle partitioning could provide a significant fraction of this missing SOA mass.

These estimates should scale directly with VROX concentrations and thus the quantity of VRVOC reactivity (k[VRVOC]). Thus, if we had assumed at the outset that parameterized non-stomatal deposition is correct and the required VRVOC reactivity was 39 % of what we have used in the HR scenario, the resulting estimate for VRVOC-derived SOA would be 0.2–$0.3\,\mu\mathrm{g\,m^{-3}}$. Similarly, a depositional loss of VROX of 35 % (following the upper-limit estimate in the previous section) would propagate directly into a lower estimate for SOA production.

3.6.3 Secondary chemistry

Even if some fraction of the compounds represented by VROX deposit to canopy surfaces or particles, it is likely that many of the potential oxidation products remain in the gas-phase (Holzinger et al., 2005). How these oxidized VOCs perturb the chemical system is highly dependent on their composition and concentration, both of which are obviously unknown at this stage. Nonetheless, by drawing analogies between VRVOC and known reactive BVOCs, such as monoterpenes and sesquiterpenes, we may still gain some insight into the nature and chemistry of these postulated oxidized compounds.

Some of the products that evolve during VRVOC oxidation likely include small-chain (1 to 3 carbons) carbonyl compounds. Commonly-identified molecules in terpene oxidation studies include formaldehyde (HCHO), acetaldehyde, acetone, acetic acid and formic acid (Lee et al., 2006a, b), with product yields that range from a few percent to >100 %. Of particular interest for the current study is HCHO production, as observations of anomalously high HCHO concentrations during BEARPEX-2007 suggest a substantial unidentified HCHO source at BFRS (Choi et al., 2010). First-generation HCHO yields from terpene ozonolysis vary from 4 to 80 %, with increasing yields from molecules with external double-bonds (Lee et al., 2006a). Combining these yields with the boundary layer-averaged VRVOC oxidation rate of 1.1 ppbv h^{-1}, we estimate a potential HCHO production rate of 0.05–0.9 ppbv h^{-1} from reactions of VRVOC. For comparison, Choi et al. (2010) derive a missing midday HCHO source of 1.1 – 1.6 ppbv h^{-1}. The latter estimate is for a different, cooler period of BEARPEX-2007 (mid-September) than our chosen simulation period (late August). Under cooler conditions, the contribution of VRVOC to HCHO production would be less than the values derived above due to decreased VRVOC emissions. A direct comparison at the appropriate time period would thus degrade agreement between our results and the observationally-inferred missing HCHO source. On the other hand, further oxidation of other VROX-type compounds, which we have not accounted for, could present an additional source of HCHO. Furthermore, as VRVOC oxidation is strongest within and immediately above the canopy, the impacts on HCHO mixing ratios would be largest here. For example, considering only the canopy airspace, the HCHO production rate from VRVOC oxidation grows to 1.8–36 ppbv h^{-1}. Such a source would likely be evident as a substantial upward flux in HCHO mixing ratios. Recent direct observations of HCHO fluxes at a similar Ponderosa pine forest indicate a noontime summer efflux of 24 pptv m s^{-1}, which is consistent with our estimated VRVOC-derived source (DiGangi et al., 2011). Fluxes of other small-chain oxidized VOC are thought to be dominated by direct emissions (Schade and Goldstein, 2001). Adding a leaf-level HCHO flux of 900 ng per gram of leaf per hour (Villanueva-Fierro et al., 2004) increases modeled canopy-top HCHO concentrations by 14 %, which is insufficient to explain the high HCHO mixing ratios observed in 2007.

VRVOC chemistry may also produce a number of larger oxidized hydrocarbons. Chamber and field studies have identified a variety of monoterpene and sesquiterpene oxidation products that retain a significant portion of the structure of the original VOC (Calogirou et al., 1999). The postulated VRVOC could contain multiple double bonds, implying that some VROX species would have additional reactive sites for ozone and could further contribute to the chemical ozone flux. The rate constant for ozonolysis of a second double bond is typically reduced by a factor of 2 to 100 relative to that for the first reaction (Atkinson and Arey, 2003; Calogirou et al., 1999); however, in-canopy VROX concentrations are also four times higher than VRVOC in the HR scenario, albeit with a weaker relative concentration gradient. Thus, VROX may compete with VRVOC as a sink for ozone, which in turn would lower the VRVOC emission rate required to match modeled and measured ozone fluxes. Figure 7 shows the results of a series of sensitivity tests where we force VROX to react with ozone with a rate constant equal to 0.1, 0.3 and 0.5 times that for VRVOC + O_3 (Table 1). In each scenario, the VRVOC emission rate is re-optimized to maintain agreement with measured ozone fluxes at $z/h = 1.25$ (Fig. 2). The required VRVOC emission rate is inversely proportional to the rate constant for VROX + O_3 but approaches an asymptote because VROX mixing ratios are ultimately dependent on VRVOC emission and oxidation rates. At best, the same chemical ozone flux can be sustained with a 30 % lower VRVOC emission rate if VROX also react rapidly with ozone.

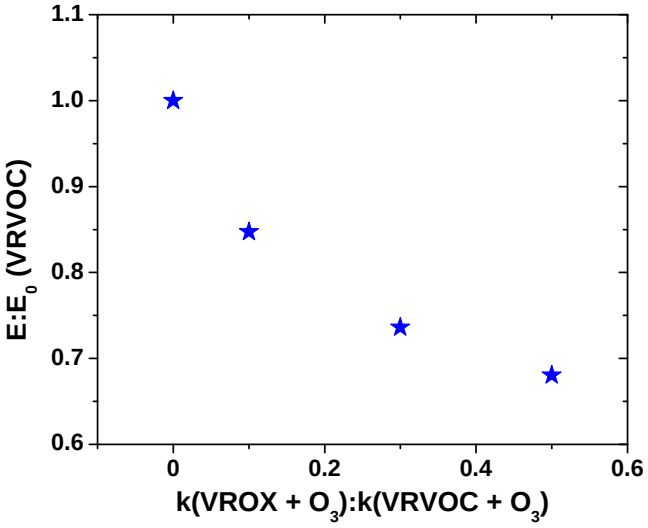

Fig. 7. Relative VRVOC emission rates required to reproduce observed non-stomatal ozone fluxes as a function of the rate constant for reaction of ozone with VROX (relative to that for reaction with VRVOC). See Sect. 3.6.3 for details.

4 Conclusions

Using a 1-D chemical-transport model of a resolved forest canopy, we have demonstrated that emissions of highly reactive but yet unidentified biogenic hydrocarbons can significantly enhance downward ozone fluxes. For the BEARPEX-2007 conditions modeled here, the entire non-stomatal component of the measured ozone flux can be explained with a VRVOC reactivity of 2×10^8 molec cm^{-3} s^{-1}, consistent with previous observational inferences for this forest. Current parameterizations of ozone deposition typically assume that non-stomatal ozone fluxes are driven by uptake to

cuticles or other heterogeneous losses. Yet, clear evidence for such processes is lacking. Our results suggest that accurate partitioning of ozone fluxes between deposition and chemistry is challenging and may depend on our understanding of BVOC emissions and photochemistry in forested regions. This work also illustrates that chemistry can perturb fluxes of reactive species even when the timescale for that chemistry is slow relative to canopy mixing, implying that a comparison of these timescales (e.g. the Damköhler number) may not be an appropriate metric for the role of chemistry in forest-atmosphere exchange.

The existence of a large chemical ozone flux carries a number of implications for chemistry within the forest. VRVOC ozonolysis may contribute as much as 1 pptv s^{-1} to OH production, which is 25 % of the total OH production rate calculated from observations during the hot period (Wolfe et al., 2011). Any model invoking a source of OH from such reactions must also account for the co-produced RO_2 to fully assess impacts on the radical budget and subsequent ozone production. Oxidized VOC resulting from this chemistry may also contribute substantially to concentrations of small-chain VOC (such as formaldehyde) or secondary organic aerosol mass, though the degree to which this occurs is highly dependent on the nature and quantity of the precursor VOCs, which is presently unknown. If the postulated compounds represented by VRVOC contain multiple double bonds, further reaction of ozone with oxidized products may reduce the magnitude of VRVOC emissions invoked from non-stomatal ozone fluxes by as much as 30 %.

Results from this study highlight key areas where additional observations are needed to constrain forest-atmosphere exchange of reactive species like ozone. A lack of detailed knowledge on the mechanisms or even expected magnitude of non-stomatal deposition is a major, though often overlooked, source of uncertainty in current-generation resistance parameterizations. Controlled experiments in both the laboratory and field should be able to provide insight on this process. Such studies would include direct ozone uptake measurements on both actual and simulated plant surfaces (e.g. Cape et al., 2009) and should take special care to minimize the confounding influence of ozone-VOC reactions. This information will allow for better constraints on chemical fluxes of ozone and other reactive species. If the quantity of VRVOC-driven ozone reactivity in the forest is as high as invoked by previous studies, we suggest that it should be observable via a bulk "ozone reactivity" measurement that quantifies the gross loss rate of ozone in a sampled air mass. Such an experiment could be carried out on ambient air in the canopy or with the effluent from a branch enclosure (Helmig et al., 2010). Modeled profiles of the ozone exchange velocity also indicate that a flux divergence measurement (e.g. measurement of the flux at two heights) could distinguish between fluxes that are predominantly depositional or chemical, although the inherent variability in eddy covariance fluxes would make this a challenging endeavor as the estimated change in ozone fluxes between $z/h = 1$ and 3 is only 30 %. Observations of RO_2 radicals are also a critical missing link when trying to assess radical budgets and cycling in areas of high BVOC emissions, and if the quantity of VRVOC-driven ozone reactivity is high then vertical gradients in RO_2 and other major products such as formaldehyde should be observable.

Acknowledgements. The authors acknowledge support from National Science Foundation grants ATM-0633897 and ATM-CAREER 0846183, and for the UC Berkeley contributions to this work ATM-0922562. GMW was partially supported by a US-EPA STAR Fellowship Assistance under Agreement No. FP-91698901. This work has not been formally reviewed by EPA. The views expressed in this work are solely those of the authors; EPA and NSF do not endorse any products or commercial services mentioned. The authors also thank Sierra Pacific Industries for the use of land, Blodgett Forest Research Station staff for cooperation during BEARPEX and two anonymous reviews for insightful feedback on the manuscript.

Edited by: A. B. Guenther

References

Altimir, N., Tuovinen, J. P., Vesala, T., Kulmala, M., and Hari, P.: Measurements of ozone removal by Scots pine shoots: calibration of a stomatal uptake model including the non-stomatal component, Atmos. Environ., 38, 2387–2398, 2004.

Altimir, N., Kolari, P., Tuovinen, J.-P., Vesala, T., Bck, J., Suni, T., Kulmala, M., and Hari, P.: Foliage surface ozone deposition: a role for surface moisture?, Biogeosciences, 3, 209–228, doi:10.5194/bg-3-209-2006, 2006.

Aschmann, S. M., Arey, J., and Atkinson, R.: OH radical formation from the gas-phase reactions of O_3 with a series of terpenes, Atmos. Environ., 36, 4347–4355, 2002.

Ashmore, M. R.: Assessing the future global impacts of ozone on vegetation, Plant Cell Environ., 28, 949–964, 2005.

Atkinson, R. and Arey, J.: Gas-phase tropospheric chemistry of biogenic volatile organic compounds: a review, Atmos. Environ., 37, S197–S219, 2003.

Baldocchi, D.: A Multi-Layer Model for Estimating Sulfur Dioxide Deposition to a Deciduous Oak Forest Canopy, Atmos. Environ., 22, 869–884, 1988.

Bassin, S., Calanca, P., Weidinger, T., Gerosa, G., and Fuhrer, E.: Modeling seasonal ozone fluxes to grassland and wheat: model improvement, testing, and application, Atmos. Environ., 38, 2349–2359, 2004.

Bouvier-Brown, N. C., Goldstein, A. H., Gilman, J. B., Kuster, W. C., and de Gouw, J. A.: In-situ ambient quantification of monoterpenes, sesquiterpenes, and related oxygenated compounds during BEARPEX 2007: implications for gas- and particle-phase chemistry, Atmos. Chem. Phys., 9, 5505-5518, doi:10.5194/acp-9-5505-2009, 2009a.

Bouvier-Brown, N. C., Holzinger, R., Palitzsch, K., and Goldstein, A. H.: Large emissions of sesquiterpenes and methyl chavicol quantified from branch enclosure measurements, Atmos. Environ., 43, 389–401, 2009b.

Bouvier-Brown, N. C., Schade, G. W., Misson, L., Lee, A., McKay, M., and Goldstein, A. H.: Contributions of biogenic volatile organic compounds to net ecosystem carbon flux, J. Geophys. Res., in review, 2011.

Bytnerowicz, A. and Fenn, M. E.: Nitrogen deposition in California forests: a review, Environ. Pollut., 92, 127–146, 1996.

Bytnerowicz, A., Arbaugh, M., Schilling, S., Fraczek, W., and Alexander, D.: Ozone distribution and phytotoxic potential in mixed conifer forests of the San Bernardino Mountains, Southern California, Environ. Pollut., 155, 398–408, 2008.

Cahill, T. M., Seaman, V. Y., Charles, M. J., Holzinger, R., and Goldstein, A. H.: Secondary organic aerosols formed from oxidation of biogenic volatile organic compounds in the Sierra Nevada Mountains of California, J. Geophys. Res., 111, D16312, 10.1029/2006JD007178, 2006.

Calogirou, A., Larsen, B. R., and Kotzias, D.: Gas-phase terpene oxidation products: a review, Atmos. Environ., 33, 1423–1439, 1999.

Cantrell, C. A., Lind, J. A., Shetter, R. E., Calvert, J. G., Goldan, P. D., Kuster, W., Fehsenfeld, F. C., Montzka, S. A., Parrish, D. D., Williams, E. J., Buhr, M. P., Westberg, H. H., Allwine, G., and Martin, R.: Peroxy-radicals in the Rose experiment – measurement and theory, J. Geophys. Res.-Atmos., 97, 20671–20686, 1992.

Cape, J. N., Hamilton, R., and Heal, M. R.: Reactive uptake of ozone at simulated leaf surfaces: Implications for 'non-stomatal' ozone flux, Atmos. Environ., 43, 1116–1123, 2009.

Choi, W., Faloona, I. C., Bouvier-Brown, N. C., McKay, M., Goldstein, A. H., Mao, J., Brune, W. H., LaFranchi, B. W., Cohen, R. C., Wolfe, G. M., Thornton, J. A., Sonnenfroh, D. M., and Millet, D. B.: Observations of elevated formaldehyde over a forest canopy suggest missing sources from rapid oxidation of arboreal hydrocarbons, Atmos. Chem. Phys., 10, 8761–8781, doi:10.5194/acp-10-8761-2010, 2010.

Coe, H., Gallagher, M. W., Choularton, T. W., and Dore, C.: Canopy Scale Measurements Of Stomatal And Cuticular O_3 Uptake By Sitka Spruce, Atmos. Environ., 29, 1413–1423, 1995.

Darrall, N. M.: The effect of air pollutants on physiological processes in plants, Plants, Cell and Environment, 12, 1–30, 1989.

DiGangi, J. P., Boyle, E. S., Karl, T., Harley, P., Turnipseed, A., Kim, S., Cantrell, C., Maudlin III, R. L., Zheng, W., Flocke, F., Hall, S. R., Ullmann, K., Nakashima, Y., Paul, J. B., Wolfe, G. M., Desai, A. R., Kajii, Y., Guenther, A., and Keutsch, F. N.: First direct measurements of formaldehyde flux via eddy covariance: implications for missing in-canopy formaldehyde sources, Atmos. Chem. Phys. Discuss., 11, 18729–18766, doi:10.5194/acpd-11-18729-2011, 2011.

Dillon, M. B., Lamanna, M. S., Schade, G. W., Goldstein, A., and Cohen, R. C.: Chemical evolution of the Sacramento urban plume: Transport and oxidation, J. Geophys. Res., 107, 4045, 10.1029/2001JD000969, 2002.

Dorsey, J. R., Duyzer, J. H., Gallagher, M. W., Coe, H., Pilegaard, K., Weststrate, J. H., Jensen, N. O., and Walton, S.: Oxidized nitrogen and ozone interaction with forests. I: Experimental observations and analysis of exchange with Douglas fir, Q. J. Roy. Meteor. Soc., 130, 1941–1955, 2004.

Duyzer, J. H., Dorsey, J. R., Gallagher, M. W., Pilegaard, K., and Walton, S.: Oxidized nitrogen and ozone interaction with forests. II: Multi-layer process-oriented modelling results and a sensitivity study for Douglas fir, Q. J. Roy. Meteor. Soc., 130, 1957–1971, 2004.

Faloona, I., Tan, D., Brune, W., Hurst, J., Barket, D., Couch, T. L., Shepson, P., Apel, E., Riemer, D., Thornberry, T., Carroll, M. A., Sillman, S., Keeler, G. J., Sagady, J., Hooper, D., and Paterson, K.: Nighttime observations of anomalously high levels of hydroxyl radicals above a deciduous forest canopy, J. Geophys. Res.-Atmos., 106, 24315–24333, 2001.

Fares, S., McKay, M., Holzinger, R., and Goldstein, A. H.: Ozone fluxes in a Pinus ponderosa ecosystem are dominated by non-stomatal processes: Evidence from long-term continuous measurements, Agr. Forest Meteorol., 150, 42–431, 2010a.

Fares, S., Park, J. H., Ormeno, E., Gentner, D. R., McKay, M., Loreto, F., Karlik, J., and Goldstein, A. H.: Ozone uptake by citrus trees exposed to a range of ozone concentrations, Atmos. Environ., 44, 3404–3412, 2010b.

Farmer, D. K. and Cohen, R. C.: Observations of HNO_3, ΣAN, ΣPN and NO_2 fluxes: evidence for rapid HO_x chemistry within a pine forest canopy, Atmos. Chem. Phys., 8, 3899–3917, doi:10.5194/acp-8-3899-2008, 2008.

Farmer, D. K., Kimmel, J. R., Phillips, G., Docherty, K. S., Worsnop, D. R., Sueper, D., Nemitz, E., and Jimenez, J. L.: Eddy covariance measurements with high-resolution time-of-flight aerosol mass spectrometry: a new approach to chemically resolved aerosol fluxes, Atmos. Meas. Tech., 4, 1275–1289, doi:10.5194/amt-4-1275-2011, 2011.

Fowler, D., Pilegaard, K., Sutton, M. A., Ambus, P., Raivonen, M., Duyzer, J., Simpson, D., Fagerli, H., Fuzzi, S., Schjoerring, J. K., Granier, C., Neftel, A., Isaksen, I. S. A., Laj, P., Maione, M., Monks, P. S., Burkhardt, J., Daemmgen, U., Neirynck, J., Personne, E., Wichink-Kruit, R., Butterbach-Bahl, K., Flechard, C., Tuovinen, J. P., Coyle, M., Gerosa, G., Loubet, B., Altimir, N., Gruenhage, L., Ammann, C., Cieslik, S., Paoletti, E., Mikkelsen, T. N., Ro-Poulsen, H., Cellier, P., Cape, J. N., Horvath, L., Loreto, F., Niinemets, U., Palmer, P. I., Rinne, J., Misztal, P., Nemitz, E., Nilsson, D., Pryor, S., Gallagher, M. W., Vesala, T., Skiba, U., Brueggemann, N., Zechmeister-Boltenstern, S., Williams, J., O'Dowd, C., Facchini, M. C., de Leeuw, G., Flossman, A., Chaumerliac, N., and Erisman, J. W.: Atmospheric composition change: Ecosystems-Atmosphere interactions, Atmos. Environ., 43, 5193–5267, 2009.

Gao, W., Wesely, M. L., and Doskey, P. V.: Numerical modeling of the turbulent diffusion and chemistry of NO_x, O_3, isoprene, and other reactive trace gases in and above a forest canopy, J. Geophys. Res., 98, 18339–18353, 1993.

Glowacki, D. R. and Pilling, M. J.: Unimolecular Reactions of Peroxy Radicals in Atmospheric Chemistry and Combustion, Chemphyschem, 11, 3836–3843, 2010.

Goldstein, A. H., Hultman, N. E., Fracheboud, J. M., Bauer, M. R., Panek, J. A., Xu, M., Qi, Y., Guenther, A. B., and Baugh, W.: Effects of climate variability on the carbon dioxide, water, and sensible heat fluxes above a ponderosa pine plantation in the Sierra Nevada (CA), Agr. Forest Meteorol., 101, 113–129, 2000.

Goldstein, A. H., McKay, M., Kurpius, M. R., Schade, G. W., Lee, A., Holzinger, R., and Rasmussen, R. A.: Forest thinning experiment confirms ozone deposition to forest canopy is dominated by reaction with biogenic VOCs, Geophys. Res. Lett., 31, L22106, 10.1029/2004GL021259, 2004.

Goumenaki, E., Taybi, T., Borland, A., and Barnes, J.: Mechanisms

underlying the impacts of ozone on photosynthetic performance, Environmental And Experimental Botany, 69, 259–266, 2010.

Guenther, A., Hewitt, C. N., Erickson, D., Fall, R., Geron, C., Graedel, T., Harley, P., Klinger, L., Lerdau, M. T., McKay, W. A., Pierce, T., Scholes, B., Steinbrecher, R., Tallamraju, R., Taylor, J., and Zimmerman, P.: A global model of natural volatile organic compound emissions, J. Geophys. Res., 100, 8873–8892, 1995.

Hallquist, M., Wenger, J. C., Baltensperger, U., Rudich, Y., Simpson, D., Claeys, M., Dommen, J., Donahue, N. M., George, C., Goldstein, A. H., Hamilton, J. F., Herrmann, H., Hoffmann, T., Iinuma, Y., Jang, M., Jenkin, M. E., Jimenez, J. L., Kiendler-Scharr, A., Maenhaut, W., McFiggans, G., Mentel, Th. F., Monod, A., Prévôt, A. S. H., Seinfeld, J. H., Surratt, J. D., Szmigielski, R., and Wildt, J.: The formation, properties and impact of secondary organic aerosol: current and emerging issues, Atmos. Chem. Phys., 9, 5155–5236, doi:10.5194/acp-9-5155-2009, 2009.

Helmig, D., Daly, R., and Bertman, S. B.: Ozone reactivity of biogenic volatile organic compounds emitted from the four dominant tree species at PROPHET - CABINEX, AGU Fall Meeting, San Francisco, CA, 2010, Abstract A53C-0240,

Herrmann, F., Winterhalter, R., Moortgat, G. K., and Williams, J.: Hydroxyl radical (OH) yields from the ozonolysis of both double bonds for five monoterpenes, Atmos. Environ., 44, 3458–3464, 2010.

Hogg, A., Uddling, J., Ellsworth, D., Carroll, M. A., Pressley, S., Lamb, B., and Vogel, C.: Stomatal and non-stomatal fluxes of ozone to a northern mixed hardwood forest, Tellus B, 59, 514–525, 2007.

Holzinger, R., Lee, A., Paw, K. T., and Goldstein, U. A. H.: Observations of oxidation products above a forest imply biogenic emissions of very reactive compounds, Atmos. Chem. Phys., 5, 67–75, doi:10.5194/acp-5-67-2005, 2005.

Jenkin, M. E., Saunders, S. M., and Pilling, M. J.: The tropospheric degradation of volatile organic compounds: A protocol for mechanism development, Atmos. Environ., 31, 81–104, 1997.

Karl, T., Harley, P., Guenther, A., Rasmussen, R., Baker, B., Jardine, K., and Nemitz, E.: The bi-directional exchange of oxygenated VOCs between a loblolly pine (*Pinus taeda*) plantation and the atmosphere, Atmos. Chem. Phys., 5, 3015–3031, doi:10.5194/acp-5-3015-2005, 2005.

Karl, T., Harley, P., Emmons, L., Thornton, B., Guenther, A., Basu, C., Turnipseed, A., and Jardine, K.: Efficient Atmospheric Cleansing of Oxidized Organic Trace Gases by Vegetation, Science, 330, 816–819, 2010.

Karnosky, D. F., Mankovska, B., Percy, K., Dickson, R. E., Podila, G. K., Sober, J., Noormets, A., Hendrey, G., Coleman, M. D., Kubiske, M., Pregitzer, K. S., and Isebrands, J. G.: Effects of tropospheric O_3 on trembling aspen and interaction with CO2: Results from an O_3-gradient and a face experiment, Water Air Soil Poll., 116, 311–322, 1999.

Kurpius, M. R. and Goldstein, A. H.: Gas-phase chemistry dominates O_3 loss to a forest, implying a source of aerosols and hydroxyl radicals to the atmosphere, Geophys. Res. Lett., 30, 1371–1374, 10.1029/2002GL016785, 2003.

LaFranchi, B. W., Wolfe, G. M., Thornton, J. A., Harrold, S. A., Browne, E. C., Min, K. E., Wooldridge, P. J., Bilman, J. B., Kuster, W. C., Goldan, P. D., de Gouw, J. A., McKay, M., Goldstein, A. H., Ren, X., Mao, J., and Cohen, R. C.: Closing the peroxy acetyl nitrate budget: observations of acyl peroxy nitrates (PAN, PPN, and MPAN) during BEARPEX 2007, Atmos. Chem. Phys., 9, 7623-7641, 2009, http://www.atmos-chem-phys.net/9/7623/2009/.

Lee, A., Goldstein, A. H., Keywood, M. D., Gao, S., Varutbangkul, V., Bahreini, R., Ng, N. L., Flagan, R. C., and Seinfeld, J. H.: Gas-phase products and secondary aerosol yields from the ozonolysis of ten different terpenes, J. Geophys. Res., 111, 1–18, doi:10.1029/2005JD006437, 2006a.

Lee, A., Goldstein, A. H., Kroll, J. H., Ng, N. L., Varutbangkul, V., Flagan, R. C., and Seinfeld, J. H.: Gas-phase products and secondary aerosol yields from the photooxidation of 16 different terpenes, J. Geophys. Res., 111, 1–25, 10.1029/2006JD007050, 2006b.

Matyssek, R., and Innes, J. L.: Ozone – A risk factor for trees and forests in Europe?, Water Air Soil Poll., 116, 199–226, 1999.

Matyssek, R., Wieser, G., Ceulemans, R., Rennenberg, H., Pretzsch, H., Haberer, K., Low, M., Nunn, A. J., Werner, H., Wipfler, P., Osswaldg, W., Nikolova, P., Hanke, D. E., Kraigher, H., Tausz, M., Bahnweg, G., Kitao, M., Dieler, J., Sandermann, H., Herbinger, K., Grebenc, T., Blumenrother, M., Deckmyn, G., Grams, T. E. E., Heerdt, C., Leuchner, M., Fabian, P., and Haberle, K. H.: Enhanced ozone strongly reduces carbon sink strength of adult beech (Fagus sylvatica) – Resume from the free-air fumigation study at Kranzberg Forest, Environ. Pollut., 158, 2527-2-532, 2010.

Monteith, J. L. and Unsworth, M. H.: Principles of Environmental Physics, 2nd ed., Edward Arnold, London, UK, 1990.

Paulson, S. E., Chung, M., Sen, A. D., and Orzechowska, G.: Measurement of OH radical formation from the reaction of ozone with several biogenic alkenes, J. Geophys. Res.-Atmos., 103, 25533–25539, 1998.

Paulson, S. E., Chung, M. Y., and Hasson, A. S.: OH radical formation from the gas-phase reaction of ozone with terminal alkenes and the relationship between structure and mechanism, J. Phys. Chem. A, 103, 8125–8138, 1999.

Perring, A. E., Bertram, T. H., Wooldridge, P. J., Fried, A., Heikes, B. G., Dibb, J., Crounse, J. D., Wennberg, P. O., Blake, N. J., Blake, D. R., Brune, W. H., Singh, H. B., and Cohen, R. C.: Airborne observations of total $RONO_2$: new constraints on the yield and lifetime of isoprene nitrates, Atmos. Chem. Phys., 9, 1451–1463, doi:10.5194/acp-9-1451-2009, 2009.

Qi, B., Takami, A., and Hatakeyama, S.: Peroxy radical concentrations measured at a forest canopy in Nikko, Japan, in summer 2002, J. Atmos. Chem., 52, 63–79, 2005.

Raupach, M. R.: A practical Lagrangian method for relating scalar concentrations to source distributions in vegetation canopies, Q. J. Roy. Meteor. Soc., 115, 609–632, 1989.

Rollins, A. W., Kiendler-Scharr, A., Fry, J. L., Brauers, T., Brown, S. S., Dorn, H.-P., Dubé, W. P., Fuchs, H., Mensah, A., Mentel, T. F., Rohrer, F., Tillmann, R., Wegener, R., Wooldridge, P. J., and Cohen, R. C.: Isoprene oxidation by nitrate radical: alkyl nitrate and secondary organic aerosol yields, Atmos. Chem. Phys., 9, 6685–6703, doi:10.5194/acp-9-6685-2009, 2009.

Rondon, A., Johansson, C., and Granat, L.: Dry Deposition Of Nitrogen-Dioxide And Ozone To Coniferous Forests, J. Geophys. Res.-Atmos., 98, 5159–5172, 1993.

Saunders, S. M., Jenkin, M. E., Derwent, R. G., and Pilling, M.

J.: Protocol for the development of the Master Chemical Mechanism, MCM v3 (Part A): tropospheric degradation of non-aromatic volatile organic compounds, Atmos. Chem. Phys., 3, 161–180, doi:10.5194/acp-3-161-2003, 2003.

Schade, G. W. and Goldstein, A. H.: Fluxes of oxygenated volatile organic compounds from a ponderosa pine plantation, J. Geophys. Res., 106, 3111–3123, 2001.

Schade, G. W. and Goldstein, A. H.: Plant physiological influences on the fluxes of oxygenated volatile organic compounds from ponderosa pine trees, J. Geophys. Res.-Atmos., 107, 4082–4091, 2002.

Schwede, D., Zhang, L., Vet, R., and Lear, G.: An intercomparison of the deposition models used in the CASTNET and CAPMoN networks, Atmos. Environ., 45, 1337–1346, doi:10.1016/j.atmosenv.2010.11.050, 2011.

Shu, Y. and Atkinson, R.: Rate Constants for the Gas-Phase Reactions of O_3 with a Series of Terpenes and OH Radical Formation from the O_3 Reactions with Sesquiterpenes at 296 ± 2 K, Int. J. Chem. Kinet., 26, 1193–1205, 1994.

Stevenson, D. S., Dentener, F. J., Schultz, M. G., Ellingsen, K., van Noije, T. P. C., Wild, O., Zeng, G., Amann, M., Atherton, C. S., Bell, N., Bergmann, D. J., Bey, I., Butler, T., Cofala, J., Collins, W. J., Derwent, R. G., Doherty, R. M., Drevet, J., Eskes, H. J., Fiore, A. M., Gauss, M., Hauglustaine, D. A., Horowitz, L. W., Isaksen, I. S. A., Krol, M. C., Lamarque, J. F., Lawrence, M. G., Montanaro, V., Muller, J. F., Pitari, G., Prather, M. J., Pyle, J. A., Rast, S., Rodriguez, J. M., Sanderson, M. G., Savage, N. H., Shindell, D. T., Strahan, S. E., Sudo, K., and Szopa, S.: Multimodel ensemble simulations of present-day and near-future tropospheric ozone, J. Geophys. Res.-Atmos., 111, D08301, doi:10.1029/2005JD006338, 2006.

Stroud, C., Makar, P., Karl, T., Guenther, A., Geron, C., Turnipseed, A. A., Nemitz, E., Baker, B., Potosnak, M., and Fuentes, J. D.: Role of canopy-scale photochemistry in modifying biogenic-atmosphere exchange of reactive terpenoid species: Results from the CELTIC field study, J. Geophys. Res., 110, D17303, 10.1029/2005JD005775, 2005.

Tan, D., Faloona, I., Simpas, J. B., Brune, W., Shepson, P. B., Couch, T. L., Sumner, A. L., Carroll, M. A., Thornberry, T., Apel, E., Riemer, D., and Stockwell, W.: HOx budgets in a deciduous forest: Results from the PROPHET summer 1998 campaign, J. Geophys. Res.-Atmos., 106, 24407–24427, 2001.

Thom, A. S.: Momentum, mass and heat exchange of plant communities, in: Vegetation and Atmosphere, edited by: Monteith, J. L., Elsevier, New York, NY, 57–109, 1975.

UNECE: Manual on methodologies and criteria for modelling and mapping critical loads & levels and air pollution effects, risks and trends, available at: www.icpmapping.org, 2004.

Villanueva-Fierro, I., Popp, C. J., and Martin, R. S.: Biogenic emissions and ambient concentrations of hydrocarbons, carbonyl compounds and organic acids from ponderosa pine and cottonwood trees at rural and forested sites in Central New Mexico, Atmos. Environ., 38, 249–260, 2004.

Walton, S., Gallagher, M. W., and Duyzer, J. H.: Use of a detailed model to study the exchange of NO_x and O_3 above and below a deciduous canopy, Atmos. Environ., 31, 2915–2931, 1997.

Wesely, M. L.: Parameterization of surface resistances to gaseous dry deposition in regional-scale numerical models, Atmos. Environ., 23, 1293–1304, 1989.

Wesely, M. L. and Hicks, B. B.: A review of the current status of knowledge on dry deposition, Atmos. Environ., 34, 2261–2282, 2000.

Winterhalter, R., Herrmann, F., Kanawati, B., Nguyen, T. L., Peeters, J., Vereecken, L., and Moortgat, G. K.: The gas-phase ozonolysis of beta-caryophyllene (C15H24). Part I: an experimental study, Phys. Chem. Chem. Phys., 11, 4152–4172, 2009.

Wolfe, G. M. and Thornton, J. A.: The Chemistry of Atmosphere-Forest Exchange (CAFE) Model - Part 1: Model description and characterization, Atmos. Chem. Phys., 11, 77–101, doi:10.5194/acp-11-77-2011, 2011.

Wolfe, G. M., Thornton, J. A., Bouvier-Brown, N. C., Goldstein, A. H., Park, J.-H., McKay, M., Matross, D. M., Mao, J., Brune, W. H., LaFranchi, B. W., Browne, E. C., Min, K.-E., Wooldridge, P. J., Cohen, R. C., Crounse, J. D., Faloona, I. C., Gilman, J. B., Kuster, W. C., de Gouw, J. A., Huisman, A., and Keutsch, F. N.: The Chemistry of Atmosphere-Forest Exchange (CAFE) Model - Part 2: Application to BEARPEX-2007 observations, Atmos. Chem. Phys., 11, 1269–1294, doi:10.5194/acp-11-1269-2011, 2011.

Yi, C.: Momentum Transfer within Canopies, J. Appl. Meteorol. Clim., 47, 262–275, 10.1175/2007JAMC1667.1, 2008.

Zapletal, M., Cudlin, P., Chroust, P., Urban, O., Pokorny, R., Edwards-Jonasova, M., Czerny, R., Janous, D., Taufarova, K., Vecera, Z., Mikuska, P., and Paoletti, E.: Ozone flux over a Norway spruce forest and correlation with net ecosystem production, Environ. Pollut., 159, 1024–1034, 2011.

Zhang, L., Brook, J. R., and Vet, R.: A revised parameterization for gaseous dry deposition in air-quality models, Atmos. Chem. Phys., 3, 2067–2082, doi:10.5194/acp-3-2067-2003, 2003.

Zhang, L. M., Brook, J. R., and Vet, R.: On ozone dry deposition – with emphasis on non-stomatal uptake and wet canopies, Atmos. Environ., 36, 4787–4799, 2002.

Zheng, Y., Shimizu, H., and Barnes, J. D.: Limitations to CO_2 assimilation in ozone-exposed leaves of plantago major, New Phytologist, 155, 67–68, 2002.